

Silicon-Bridged Alkali-Metal and Alkaline-Earth-Metal Metallocene Complexes

Sjoerd Harder,* Martin Lutz, and Alfred W. G. Straub

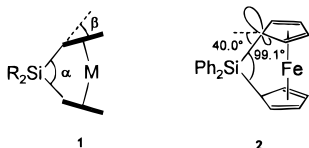
Universität Konstanz, Postfach 5560, M738, D-78434 Konstanz, Germany

Received July 16, 1996[®]

The crystal structures of Si-bridged fluorenyl metallocenes with several alkali or alkaline-earth metals have been determined. $\text{Me}_2\text{Si}(\text{Fl})_2\text{Li}_2$ (Fl = fluorenyl) crystallizes from THF as a solvent-separated ion pair: $[\text{Me}_2\text{SiFl}_2\text{Li}\cdot 2\text{THF}]^- [\text{Li}\cdot 4\text{THF}]^+$. The Li^+ cation encapsulated by $\text{Me}_2\text{SiFl}_2^{2-}$ is bonded to both fluorenyl rings in an η^1 -fashion. The structure of $\text{Me}_2\text{SiFl}_2\text{-Ca}\cdot 3\text{THF}$ shows η^3 -bonding of both fluorenyl rings to Ca. The analogous Ba compound crystallizes as a tetrakis-THF solvate $\text{Me}_2\text{SiFl}_2\text{Ba}\cdot 4\text{THF}$. The unit cell contains two independent molecules with different Ba coordination geometries, (η^5 , η^3) in one and (η^3 , η^3) in the other. The structures of the Si-bridged fluorenyl metallocenes reported here do not show the distortions that are typical for Si-bridged d- and f-block metallocenes. No squeezing of the $\text{C}_{\text{ipso}}\text{-Si-C}_{\text{ipso}}$ angles and tilting of the fluorenyl ring toward the metal are observed. Instead, the fluorenyl rings tilt away from the metal in order to create room for a more extended solvation of the cation by THF.

Introduction

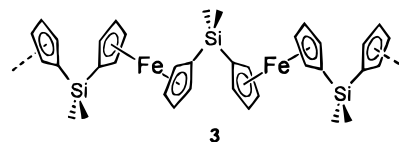
Silicon-bridged metallocenes of the d- and f-block metals are widely used in homogeneous Ziegler–Natta polymerizations¹ and catalyses.² The many structures reported for such Si-bridged metallocenes³ have one characteristic feature in common: a typical distortion of the R_2SiCp_2 ligand (see 1). The Cp–Si–Cp angle in



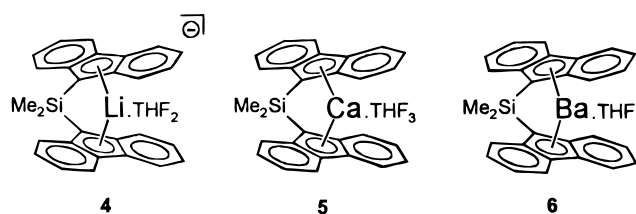
a fully relaxed R_2SiCp_2 ligand is too large for efficient metal chelation. Effective $\text{R}_2\text{SiCp}_2\text{-M}$ bonding is obtained by: (i) squeezing of the Cp–Si–Cp angle (α in 1) and (ii) tilting of the Cp plane in respect to the Si– C_{ipso} axis (β in 1).

Deformations are most the extreme for R_2SiCp_2 ligands encapsulating small metals like Fe: e.g., $\text{Ph}_2\text{SiCp}_2\text{Fe}$ (2) shows squeeze and tilt angles $\alpha = 40.0^\circ$ and $\beta = 99.1^\circ$, respectively.^{3b} Geometrically, the Cp–Fe bond is described as an (η^5)Cp–Fe interaction with five similar C–Fe bond lengths. However, the geometry around the Si bonded C_{ipso} is close to sp^3 . Therefore, the Cp–Fe bonding in such systems should be considered to be distorted toward an (η^4)Cp–Fe interaction. Such highly strained ferrocenophanes easily ring open

to form polymer strings which allow for strain-free (η^5)Cp–Fe bonding (3).⁴



Although Si-bridged main group metallocene complexes are the precursors for many d- and f-block metallocenes, no structural investigations of these systems have been reported hitherto. Here we describe the structures of the $\text{Me}_2\text{Si}(\text{fluorenyl})_2^{2-}$ ligand encapsulating an alkali or alkaline-earth metal (4–6).



The fluorenyl group can be considered as a large substituted Cp moiety with an extended π -system. It also offers suitable coordinative properties for the larger electropositive metals. This allows for a comparison between Si-bridged metallocenes with metals having a variety of sizes.

Structure of $[\text{Me}_2\text{Si}(\text{fluorenyl})_2\text{Li}\cdot 2\text{THF}]^-$. $\text{Me}_2\text{Si}(\text{fluorenyl})_2\text{Li}_2$ ($\text{Me}_2\text{SiFl}_2\text{Li}_2$) crystallizes from THF as a solvent separated ion pair: $[\text{Me}_2\text{SiFl}_2\text{Li}\cdot 2\text{THF}]^- [\text{Li}\cdot 4\text{THF}]^+$ (Figure 1; selected bond distances and angles in Table 1). Both fluorenyl ligands show (η^1)-Fl–Li bonding. The fluorenyl $\text{C}_{\text{ipso}}\text{-Li}$ bond distances of 2.353(8) and 2.399(8) Å are slightly longer than the

(4) (a) Seyferth, D.; Withers, H. P., Jr. *Organometallics* **1982**, *1*, 1275. (b) Withers, H. P., Jr.; Seyferth, D.; Fellmann, J. D.; Garron, P. E.; Martin, S. *Organometallics* **1982**, *1*, 1283. (c) Manners, I. *Adv. Organomet. Chem.* **1995**, *37*, 131.

[®] Abstract published in *Advance ACS Abstracts*, November 15, 1996.

(1) (a) Brintzinger, H.-H.; Fischer, D.; Mülhaupt, R.; Rieger, B.; Waymouth, R. M. *Angew. Chem., Int. Ed. Engl.* **1995**, *34*, 1143. (b) Bochmann, M. *J. Chem. Soc., Dalton Trans.* **1996**, 255.

(2) (a) Fendrick, C. M.; Mintz, E. A.; Schertz, C. D.; Marks, T. J. *Organometallics* **1984**, *3*, 819. (b) Piers, W. E.; Shapiro, P. J.; Bunel, E. E.; Bercaw, J. E. *Synlett* **1990**, 74. (c) Hoveyda, A. H.; Morken, J. P. *Angew. Chem.* **1996**, *108*, 1343.

(3) (a) Köpf, H.; Pickardt, J. *Z. Naturforsch.* **1981**, *36b*, 1208. (b) Stoeckli-Evans, H.; Osborne, A. G.; Whiteley, R. H. *Helv. Chim. Acta* **1976**, *59*, 2402. (c) Hortmann, K.; Brintzinger, H.-H. *New J. Chem.* **1992**, *16*, 51. (d) Fendrick, C. M.; Schertz, L. D.; Day, V. W.; Marks, T. J. *Organometallics* **1988**, *7*, 1828. (e) Jeske, G.; Schock, L. E.; Swepton, P. N.; Schumann, H.; Marks, T. J. *J. Am. Chem. Soc.* **1985**, *107*, 8103.

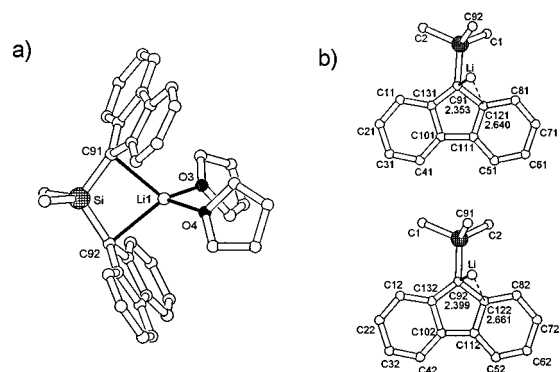
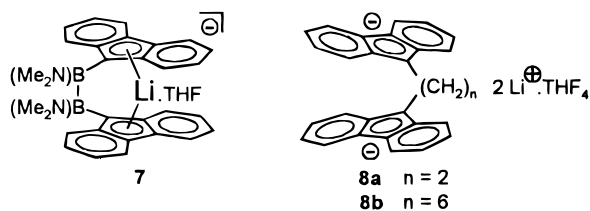


Figure 1. (a) Structure of the anion $[\text{Me}_2\text{Si}(\text{fluorenyl})_2\text{Li}\cdot 2\text{THF}]^-$. (b) Projections of the partial structures on both fluorenyl ring planes showing the atom numbering and Li coordination.

Table 1. Selected Bond Distances (Å) and Angles (deg) for $[\text{Me}_2\text{Si}(\text{fluorenyl})_2\text{Li}\cdot 2\text{THF}]^-$

C91–C121	1.451(6)	C92–C122	1.429(6)
C91–C131	1.434(6)	C92–C132	1.438(6)
C121–C111	1.427(5)	C122–C112	1.443(5)
C101–C111	1.430(6)	C102–C112	1.423(6)
C101–C131	1.440(6)	C102–C132	1.447(6)
C91–Si	1.851(4)	C92–Si	1.855(4)
Li1–C91	2.353(8)	Li1–C92	2.399(8)
Li1–C121	2.640(8)	Li1–C122	2.661(8)
Li1–O7	1.944(8)	Li1–O4	1.935(8)
C131–C91–C121	104.6(3)	C132–C92–C122	105.6(3)
Si–C91–C121	124.5(3)	Si–C92–C122	126.1(3)
Si–C91–C131	130.6(3)	Si–C92–C132	128.2(3)
C91–Si–C92	110.8(2)	C91–Li1–C92	79.9(2)
O3–Li1–O4	94.8(3)	O3–Li1–C91	114.7(3)
O4–Li1–C92	113.5(3)	O3–Li1–C92	129.5(4)
O4–Li1–C91	128.6(4)		

C–Li distance of 2.332 Å in $(\eta^1)\text{FlLi}\cdot 2\text{quinuclidine}$.⁵ The next shortest C–Li distances in **4** are quite long, 2.640(8) and 2.661(8) Å. Both fluorenyl rings are planar (the largest deviations from the least-square planes are 0.028 and 0.039 Å). The angles between Si–C_{ipso} and the fluorenyl planes measure 2.5° and 5.2° (both fluorenyl groups slightly bend away from Li). Another reported bridged fluorenyllithium compound, **7**, also crystallizes from THF as a solvent-separated ion pair.⁶



The fluorenyl rings in **7** are bonded η^2 to Li with C–Li bonds ranging from 2.212 to 2.403 Å. The longer $(\text{Me}_2\text{N})\text{B}-(\text{Me}_2\text{N})\text{B}$ bridge in **7** results in a more extended shielding of the Li^+ ion, leaving room for only one THF solvent molecule. Other bridged fluorenyllithium compounds include **8a** and **8b** which both crystallize from THF as completely solvent-separated ion pairs.⁷

(5) Brooks, J. J.; Rhine, W.; Stucky, G. D. *J. Am. Chem. Soc.* **1972**, *94*, 7339.

(6) Littger, R.; Metzler, N.; Nöth, H.; Wagner, M. *Chem. Ber.* **1994**, *127*, 1901.

(7) Becker, B.; Enkelmann, V.; Müllen, K. *Angew. Chem., Int. Ed. Engl.* **1989**, *28*, 458.

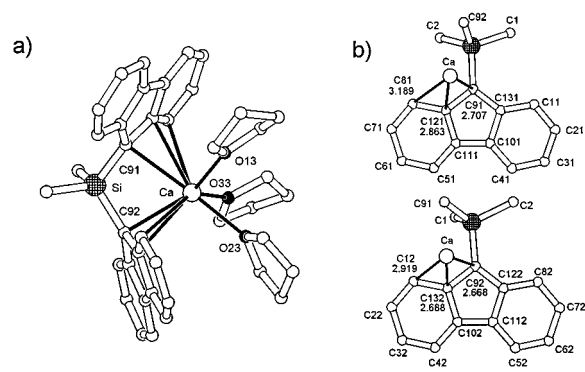
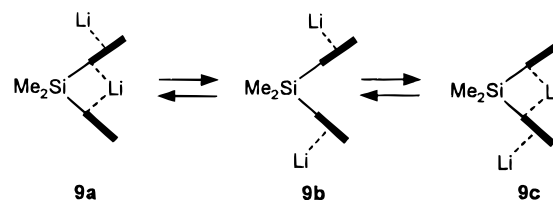


Figure 2. (a) Structure of $\text{Me}_2\text{Si}(\text{fluorenyl})_2\text{Ca}\cdot 3\text{THF}$. (b) Projections of the partial structures on both fluorenyl ring planes showing atom numbering and Ca coordination.

Crystals of $[\text{Me}_2\text{SiFl}_2\text{Li}\cdot 2\text{THF}]^-[\text{Li}\cdot 4\text{THF}]^+$ dissolve very well in toluene. In this solvent, low-temperature ^7Li NMR spectra have been recorded in order to check whether the solvent-separated ion pair structure observed in the solid state is present. For a solvent-separated ion pair two signals in a 1/1 ratio are to be expected: one for the relatively unshielded Li nucleus in $\text{Li}^+\cdot 4\text{THF}$ (around 0 ppm) and one at higher field for the Li nucleus sandwiched between the shielding cones of the aromatic fluorenyl rings.⁸ However, the ^7Li spectrum at -90°C shows two signals in a 2/1 ratio at -2.98 and -3.87 ppm, respectively. This can be explained by assuming a statistical distribution of the two Li^+ ions at the inside and outside positions of the $\text{Me}_2\text{SiFl}_2^{2-}$ ligand (**9a–c**); we here assume, in analogy to earlier work,⁸ that the signals for the different external Li^+ nuclei in **9a** (**9c**) and **9b** cannot be resolved and appear as a common broad signal. The sandwiched Li^+ nucleus is more shielded than the external Li^+ and resonates at lower frequency (-3.87 ppm). Warming



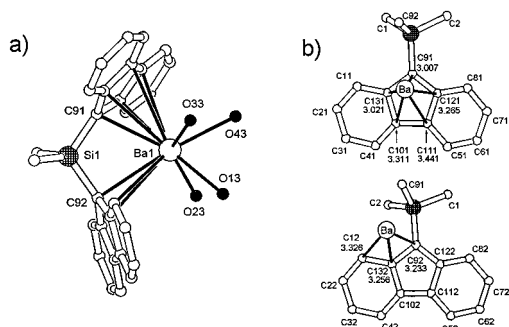
the solution results in coalescence $\delta = -3.54$ ppm, $T_{\text{coal.}} = -65^\circ\text{C}$, and $E^{\ddagger} = 9.7$ kcal/mol. Solvent-separated ion pairs might be involved in the intermediate structures for fast exchange between **9a–c**.

Structure of $\text{Me}_2\text{Si}(\text{fluorenyl})_2\text{Ca}\cdot 3\text{THF}$. $\text{Me}_2\text{SiFl}_2\text{Ca}$ crystallizes from THF as a tris-THF solvate (Figure 2; selected bond distances and angles in Table 2). Both fluorenyl groups are bonded to Ca in a distorted exocyclic η^3 -fashion with Ca–C bond distances varying from 2.668(2) to 3.189(2) Å. Each fluorenyl ring is orientated nearly eclipsed in respect to one of the Me–Si bonds. This allows for more efficient exocyclic (η^3)-Fl–Ca coordination. The fluorenyl rings are planar (the largest deviations from least-squares planes are 0.040 and 0.029 Å) and both tilt away from the Ca metal (angles between Si–C_{ipso} and the fluorenyl planes are 12.7° and 12.8°).

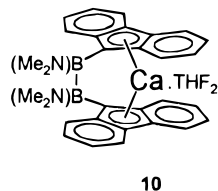
(8) (a) Paquette, L. A.; Bauer, W.; Sivik, M. R.; Bühl, M.; Feigel, M.; Schleyer, P. v. R. *J. Am. Chem. Soc.* **1990**, *112*, 8776. (b) Bauer, W.; O'Doherty, G. A.; Schleyer, P. v. R.; Paquette, L. A. *J. Am. Chem. Soc.* **1991**, *113*, 7093.

Table 2. Selected Bond Distances (Å) and Angles (deg) for Me₂Si(flourenyl)₂Ca·3THF

C91–C121	1.446(3)	C92–C122	1.453(3)
C91–C131	1.449(3)	C92–C132	1.448(3)
C121–C111	1.436(3)	C122–C112	1.430(3)
C101–C111	1.432(3)	C102–C112	1.440(3)
C101–C131	1.435(3)	C102–C132	1.434(3)
C91–Si	1.858(2)	C92–Si	1.851(2)
Ca–C91	2.707(2)	Ca–C92	2.668(2)
Ca–C121	2.863(2)	Ca–C132	2.688(2)
Ca–C81	3.189(2)	Ca–C12	2.919(2)
Ca–O13	2.319(2)	Ca–O23	2.380(2)
Ca–O33	2.333(2)		
C131–C91–C121	104.5(2)	C132–C92–C122	104.2(2)
Si–C91–C121	124.4(2)	Si–C92–C122	131.4(2)
Si–C91–C131	128.8(2)	Si–C92–C132	122.0(2)
C91–Si–C92	109.3(1)	C91–Ca–C92	68.5(1)
O13–Ca–O23	79.5(1)	O13–Ca–O33	112.7(1)
O23–Ca–O33	78.7(1)	O23–Ca–C91	161.4(1)
O23–Ca–C92	112.6(1)		

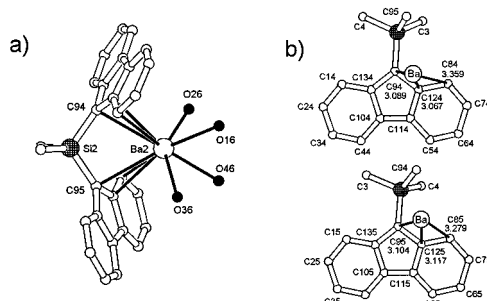
**Figure 3.** (a) Structure of one of the two independent Me₂Si(flourenyl)₂Ba·4THF molecules, the carbon atoms of THF have been omitted for clarity. (b) Projections of the partial structures on both fluorenyl ring planes showing atom numbering and Ba coordination.

An analogous (Me₂N)B–(Me₂N)B bridged compound, **10**, displays endocyclic (η^3)Fl–Ca coordination with Ca–C bond distances varying from 2.640 to 2.913 Å.⁷ The larger bridge in **10** results in more extended shielding of Ca and leaves room for only two THF solvent molecules.



Structure of Me₂Si(flourenyl)₂Ba·4THF. Me₂SiFl₂Ba crystallizes from THF as a tetrakis-THF solvate. The unit cell contains two independent molecules with different Ba coordination geometries (Figures 3 and 4; selected bond distances and angles in Table 3).

One of the Ba complexes displays (η^3)Fl–Ba and distorted (η^5)Fl–Ba coordination in which Ba–C distances vary from 3.007(4) to 3.441(4) Å (Figure 3). The fluorenyl groups are planar (largest deviations from least-squares planes are 0.033 and 0.041 Å). The fluorenyl group showing distorted (η^5)Fl–Ba bonding is slightly tilted toward the Ba metal (angle between Si–C_{ipso} and the fluorenyl plane is 4.2°) while the other is tilted away from Ba (angle between Si–C_{ipso} and the fluorenyl plane is 18.6°). The coordination sphere of Ba is completed by four THF molecules and resembles a distorted octahedron.

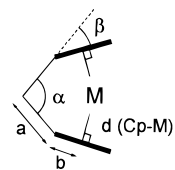
**Figure 4.** (a) Structure of one of the two independent Me₂Si(flourenyl)₂Ba·4THF molecules, the carbon atoms of THF have been omitted for clarity. (b) Projections of the partial structures on both fluorenyl ring planes showing atom numbering and Ba coordination.**Table 3. Selected Bond Distances (Å) and Angles (deg) for the Two Independent Me₂Si(flourenyl)₂Ba·4THF Molecules**

C91–C121	1.441(6)	C92–C122	1.448(6)
C91–C131	1.439(6)	C92–C132	1.444(6)
C121–C111	1.444(6)	C122–C112	1.429(6)
C101–C111	1.434(6)	C102–C112	1.438(6)
C101–C131	1.445(6)	C102–C132	1.441(5)
C91–Si1	1.857(4)	C92–Si1	1.852(4)
Ba1–C91	3.007(4)	Ba1–C92	3.233(4)
Ba1–C121	3.265(4)	Ba1–C132	3.256(4)
Ba1–C111	3.441(4)	Ba1–C12	3.326(4)
Ba1–C101	3.311(4)	Ba1–O13	2.727(3)
Ba1–C131	3.021(4)	Ba1–O23	2.726(3)
Ba1–O33	2.762(3)	Ba1–O43	2.736(3)
C131–C91–C121	105.1(3)	C132–C92–C122	104.1(3)
Si1–C91–C121	130.4(3)	Si1–C92–C122	129.8(3)
Si1–C91–C131	124.2(3)	Si1–C92–C132	122.0(3)
C91–Si1–C92	110.6(2)	C91–Ba1–C92	58.4(1)
O23–Ba1–O33	140.6(1)	O13–Ba1–O43	75.7(1)
O23–Ba1–O13	71.7(1)	O33–Ba1–O43	79.0(1)
O23–Ba1–O43	78.6(1)	O33–Ba1–O13	71.6(1)
C94–C124	1.435(5)	C95–C125	1.445(6)
C94–C134	1.443(5)	C95–C135	1.435(5)
C124–C114	1.434(5)	C125–C115	1.432(5)
C104–C114	1.431(6)	C105–C115	1.436(6)
C104–C134	1.439(6)	C105–C135	1.427(6)
C94–Si2	1.856(4)	C95–Si2	1.853(4)
Ba2–C94	3.089(4)	Ba2–C95	3.104(4)
Ba2–C124	3.067(4)	Ba2–C125	3.116(4)
Ba2–C84	3.359(4)	Ba2–C85	3.279(4)
Ba2–O16	2.779(3)	Ba2–O26	2.698(3)
Ba2–O36	2.690(3)	Ba2–O46	2.731(3)
C134–C94–C124	104.7(3)	C132–C95–C125	104.6(3)
Si2–C94–C124	124.2(3)	Si2–C95–C125	121.6(3)
Si2–C94–C134	130.9(3)	Si2–C95–C135	131.3(3)
C94–Si2–C95	111.1(2)	C94–Ba2–C95	59.2(1)
O26–Ba2–O36	145.5(1)	O16–Ba2–O46	73.1(1)
O26–Ba2–O16	84.2(1)	O36–Ba2–O46	74.2(1)
O26–Ba2–O46	73.8(1)	O36–Ba2–O16	74.4(1)

The other Ba complex, shown in Figure 4, shows double exocyclic (η^3)Fl–Ba coordination similar to that observed in Me₂SiFl₂Ca·3THF. The Ba–C bond distances vary from 3.067(4) to 3.359(4) Å. The fluorenyl rings are planar (the largest deviations from least-squares planes are 0.056 and 0.064 Å) and are both tilted away from Ba by 5.2° and 14.8°.

Both Ba complexes compare well with a recently published structure of an unbridged (fluorenyl)₂Ba·3NH₃ complex.⁹ This compound also shows a bent structure, typical for metallocenes of the heavier alka-

(9) Mösges, G.; Hampel, F.; Schleyer, P. v. R. *Organometallics* **1992**, *11*, 1769.



$$d(\text{Cp-M}) = \frac{a \cdot \sin(\alpha/2) + b \cdot \sin(\alpha/2 - \beta)}{\cos(\alpha/2 - \beta)}$$

Figure 5. Relationship between the Cp–M distance and angles α and β in *ansa*-metallocenes bridged by a single atom.

Table 4. Cp–M Distances (Å) in Monomeric $\text{R}_2\text{SiCp}_2\text{M}$ Complexes as a Function of Angles α and β (See Figure 5)

$(\eta^5)\text{Cp-M}$ ($b = 1.19 \text{ \AA}$)				
	$\alpha = 110^\circ$	$\alpha = 100^\circ$	$\alpha = 90^\circ$	$\alpha = 80^\circ$
$\beta = 0^\circ$	4.34	3.62	3.04	2.55
$\beta = 5^\circ$	3.78	3.19	2.71	2.29
$\beta = 10^\circ$	3.33	2.85	2.43	2.06
$\beta = 15^\circ$	2.98	2.56	2.20	1.87
$\beta = 20^\circ$	2.68	2.32	2.00	1.70
$(\eta^3)\text{Cp-M}$ ($b = 0.82 \text{ \AA}$)				
	$\alpha = 110^\circ$	$\alpha = 100^\circ$	$\alpha = 90^\circ$	$\alpha = 80^\circ$
$\beta = 0^\circ$	3.81	3.18	2.67	2.24
$\beta = 5^\circ$	3.33	2.82	2.40	2.03
$\beta = 10^\circ$	2.96	2.54	2.17	1.85
$\beta = 15^\circ$	2.67	2.30	1.98	1.69
$\beta = 20^\circ$	2.42	2.11	1.83	1.56
$(\eta^1)\text{Cp-M}$ ($b = 0 \text{ \AA}$)				
	$\alpha = 109^\circ$	$\alpha = 100^\circ$	$\alpha = 90^\circ$	
$\beta = 0^\circ$	2.64	2.20	1.85	
$\beta = 5^\circ$	2.36	2.00	1.71	
$\beta = 10^\circ$	2.14	1.85	1.60	

line earth metals,¹⁰ and a flexible Fl–Ba coordination geometry; also, here two independent Ba complexes with different Fl–Ba coordination geometries, η^3 , η^5 and η^5 , are observed.

Discussion

Since fluorenyl systems can be regarded as large substituted Cp systems with a more extended π -system, we will discuss the structures presented here as such.

In general, a simple formula can be derived which relates the Cp–M distance in *ansa*-metallocenes bridged by a single atom to the distortion of the ligand, *i.e.*, the angles α and β (see Figure 5). The variable a depends on the bridging atom and is circa 1.85 Å in Si-bridged metallocenes. The variable b depends on the geometry of the Cp–M coordination: for ideal (η^5 , η^3 , and η^1)-Cp–M bonding, b measures circa 1.19, 0.82, and 0 Å, respectively. Table 4a shows the combining effect of variation of angles α and β on the Cp–M distance in an (η^5 , η^5) $\text{R}_2\text{SiCp}_2\text{M}$ complex. Even the largest metal cation, Cs^+ , is too small for η^5 -complexation in a fully relaxed R_2SiCp_2 ligand (the Cp–Cs distance in the triple-decker complex $[\text{Cp}_3\text{Cs}_2]^-$ is 3.13 Å).¹¹ Thus, it is evident that Si-bridged main group metallocenes form

(10) (a) Hanusa, T. P. *Polyhedron* **1990**, *9*, 1345. (b) Hanusa, T. P. *Chem. Rev.* **1993**, *93*, 1023. (c) Burkey, D. J.; Hanusa, T. P. *Comments Inorg. Chem.* **1995**, *17*, 41. (d) Timofeeva, T. V.; Lii, J.-H.; Allinger, N. L. *J. Am. Chem. Soc.* **1995**, *117*, 7452.

(11) Harder, S.; Proscenc, M.-H. *Angew. Chem.* **1996**, *108*, 101; *Angew. Chem., Int. Ed. Engl.* **1996**, *35*, 97.

either polymers like **3** or monomers in which the Cp–metal interaction is severely distorted from ideal η^5 -bonding and/or the R_2SiCp_2 ligand is deformed as in **1**. The same holds for the structures of $\text{R}_2\text{Si}(\text{fluorenyl})_2\text{M}$ complexes. The three factors (i–iii) influencing the structures reported here are discussed below.

(i) Distortion of the R_2SiCp_2 (or R_2SiFl_2) Ligand. Squeezing of the Cp–Si–Cp angle (α) is often observed in structures of d- and f-block metallocenes. The smallest Cp–Si–Cp angle of structures included in the Cambridge Crystallographic Database¹² is $89.4(1)^\circ$ (in $\text{Me}_2\text{SiCp}_2\text{TiCl}_2$).^{3a} Such large distortion from a tetrahedral bonding geometry is relatively easily accomplished at Si. *Ab initio* calculations show that squeezing (or widening) the C–Si–C angle in Me_2SiH_2 costs only about half the energy of the analogous distortion in Me_2CH_2 (Figure 6a). The Fl–Si–Fl angles in the structures reported here (**4–6**) are all close to tetrahedral and do not show any substantial squeezing or widening: C–Si–C angles in **4**, **5**, and the two independent structures of **6** are $110.8(2)^\circ$, $109.3(1)^\circ$, $110.6(2)^\circ$, and $111.1(2)^\circ$, respectively.

Ab initio calculations also show that tilting of the Cp ring with respect to the Si–C_{ipso} axis (variation of β) in H_3SiCp^- requires only about half the energy as the analogous distortion in H_3CCp^- (Figure 6b). The geometries and natural population analysis (NPA) charges¹³ calculated for distorted and undistorted H_3CCp^- (Figure 7) show that an out-of-plane bending of the CH_3 group partially localizes the negative charge at the C_{ipso} atom. This diminished π -delocalization is also evident from the concomitant elongation of the C_{ipso}–C α and C β –C β' bonds and shortening of C α –C β bonds. However, the Si-substituted Cp rings show different behavior due to the fact that second-row elements stabilize the negative charge at a neighboring atom much better than first-row elements.¹⁴ Charges and C–C bond distances calculated for H_3SiCp^- show that even in the undistorted conformation, most of the negative charge is localized at the C_{ipso} atom. Bending the SiH₃ group out-of-plane only slightly increases the charge localization at C_{ipso}. Consequently, variation of β is more easily accomplished in H_3SiCp^- than in H_3CCp^- . Calculations on H_3SiFl^- compare very well to those on H_3SiCp^- ; in both, a nearly identical energy-bending relationship is found.

Similar analyses of the energies involved in tilting of the Cp ring in the Li complexes, H_3SiCpLi and H_3CCpLi , reveals that the direction of bending plays an important role. The bending-energy curves in Figure 6c are highly asymmetric. Bending the substituent

(12) Allen, F. H.; Kennard, O. 3D-Search and Research using the Cambridge Structural Database. *Chem. Des. Automatic News* **1993**, *8* (1), 31.

(13) Mulliken population analyses fail to give a useful and reliable characterization of the charge distribution in many cases, especially when highly ionic compounds are involved. Charges calculated according to the NPA do not show these deficiencies and are relatively basis set independent. NPA analysis: (a) Reed, A. E.; Weinstock, R. B.; Weinhold, F. *J. Chem. Phys.* **1985**, *83*, 735. (b) Reed, A. E.; Curtis, L. A.; Weinhold, F. *Chem. Rev.* **1988**, *88*, 899.

(14) (a) Lehn, J.-M.; Wipff, G. *J. Am. Chem. Soc.* **1976**, *98*, 7498. (b) Thatcher Borden, W.; Davidson, E.; Andersen, N. H.; Denniston, A. D.; Epiotis, N. D. *J. Am. Chem. Soc.* **1978**, *100*, 1604. (c) Schleyer, P. v. R.; Clark, T.; Kos, A. J.; Spitznagel, G. W.; Rohde, C.; Arad, D.; Houk, K. N.; Rondan, N. G. *J. Am. Chem. Soc.* **1984**, *106*, 6467.

(15) Lambert, C.; Schleyer, P. v. R. *Angew. Chem.* **1994**, *106*, 1187; *Angew. Chem., Int. Ed. Engl.* **1994**, *33*, 1129.

(16) Alexandratos, S.; Streitwieser, A.; Schaefer, H. F., III *J. Am. Chem. Soc.* **1976**, *98*, 7959.

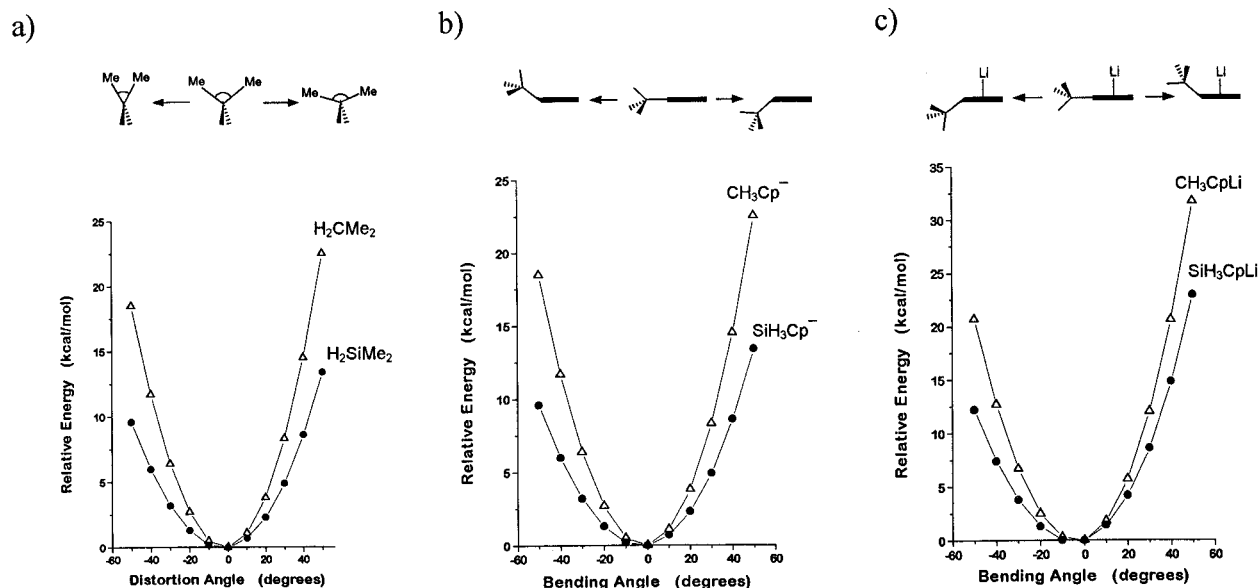


Figure 6. (a) Relative energy (*ab initio*, 6-31+G*, C_s) as a function of the distortion of the Me-C-Me or Me-Si-Me angle in H₂CMe₂ and H₂SiMe₂. (b) Relative energy (*ab initio*, 6-31+G*, C_s) as a function of bending the substituent out of the Cp plane for CH₃Cp⁻ and SiH₃Cp⁻. (c) Relative energy (*ab initio*, 6-31+G*, C_s) as a function of bending the substituent out of the Cp plane for CH₃CpLi and SiH₃CpLi.

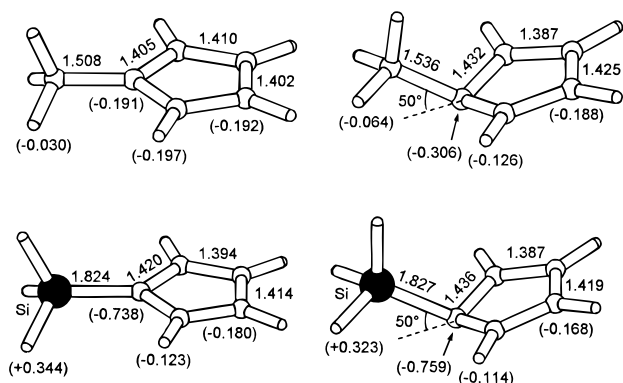


Figure 7. *Ab initio* (6-31+G*, C_s) geometries (bond lengths in Å) and group charges, *i.e.*, charge of heavy atom + attached hydrogens (given in parentheses).

away from the metal results in charge localization on the metal side (**11a**), which is more favorable than charge localization at the opposite side (**11b**).

The X-ray structures reported here display distortions in which the angle β varies from 4.2 to 18.6°. The fluorenyl rings generally bend away from the metal, and this is especially true for the largest deviations observed. Only the fluorenyl ring bonded η^5 to Ba shows a small tilting of 4.2° toward the metal. Noteworthy is the recently published structure of a Me₃Si-substituted fluorenyllithium derivative in which the 9° tilting of the Me₃Si group away from the metal is also explained in terms of Coulombic effects.^{17f,g}

(ii) Deviation from (η^5)Cp-M (or (η^5)Fl-M) Coordination. Alkali (and alkaline earth) metal-Cp

(17) (a) Hoffmann, D.; Hampel, F.; Schleyer, P. v. R. *J. Organomet. Chem.* **1993**, *13*, 456. (b) Corbelin, S.; Kopf, J.; Weiss, E. *Chem. Ber.* **1991**, *124*, 2417. (c) Johnson, J. W.; Treichel, P. M. *J. Am. Chem. Soc.* **1977**, *99*, 1427. (d) Kowala, C.; Wunderlich, J. A. *Acta Crystallogr.* **1976**, *B32*, 820. (e) Bochmann, M.; Lancaster, S. J.; Hursthouse, M. B.; Mazid, M. *Organometallics* **1993**, *12*, 4718. (f) Viebrock, H.; Aheln, D.; Weiss, E. *Z. Naturforsch.* **1994**, *B49*, 89. (g) Malaba, D.; Chen, L.; Tessier, C. A.; Youngs, W. J. *Organometallics* **1992**, *11*, 1007. (h) Malaba, D.; Djebli, A.; Chen, L.; Zarate, E. A.; Tessier, C. A.; Youngs, W. J. *Organometallics* **1993**, *12*, 1266.

bonding is largely ionic (95%)¹⁵ and has been shown to be preferably of η^5 -character.¹⁶ In R₂SiCp₂M complexes, a small deviation from the (η^5)Cp-M bonding geometry results in a large change of the Cp-M distance. Parts b and c of Table 4 show the Cp-M bond distances as a function of angles α and β in (η^3 , η^3)R₂SiCp₂M and (η^1 , η^1)R₂SiCp₂M complexes. The flexibility of anion-metal coordination in fluorenyl systems is even greater than that in the corresponding cyclopentadienyl systems: fluorenyl-metal coordination varying from η^1 to η^6 has been reported for transition metal as well as main group metal complexes.¹⁷ This rich variety of coordination modes that are observed is in accord with calculations on fluorenyllithium which show that the energy differences between the different coordination modes are less than 1.5 kcal/mol.^{17a} It is therefore not surprising that deviation from ideal η^5 -coordination is employed in order to fit the metal in the Me₂SiFl₂ ligand. Only the largest metal investigated in our studies, Ba²⁺, exhibits in one of the structures η^5 -coordination, albeit distorted. The different coordination modes found in the two crystallographically independent monomers of Me₂SiFl₂-Ba·4THF supports the fact that fluorenyl-cation coordination is highly flexible.

(iii) Solvation of the Metal Cation. Solvation plays a very important role in controlling the reactivity and structures of polar organometallic group I and II compounds.¹⁸ Energies of solvation can be considerable; *e.g.*, experimentally determined free energies involved with first, second, third, and fourth solvation of the Li cation with water are 25.5, 18.9, 13.3, and 7.5 kcal/mol, respectively.¹⁹ The number of solvent molecules filling the metal's coordination sphere depends on the steric bulk of the solvent and the space available at the empty coordination site. It is for this reason that the Si-bridged main group metallocenes reported here do not

(18) (a) Kaufmann, E.; Tidor, B.; Schleyer, P. v. R. *Organometallics* **1989**, *8*, 2577. (b) Kaufmann, E.; Raghavachari, K.; Reed, A. E.; Schleyer, P. v. R. *Organometallics* **1988**, *7*, 1597. (c) Harder, S.; Boersma, J.; van Mier, G. P. M.; Kanters, J. A.; Brandsma, L. J. *Organomet. Chem.* **1989**, *364*, 1.

(19) Džidić, I.; Kebarle, P. *J. Phys. Chem.* **1970**, *74*, 1466.

show distortions similar to those observed in Si-bridged d- and f-block metallocenes. Any squeezing of the Fl–Si–Fl angle and tilting of the fluorenyl group toward the metal results in a significant steric hindrance at the coordination site that is available for solvation. However, tilting of the fluorenyl group away from the metal, as observed in the Si-bridged main group metallocenes reported here, leads to an extension of solvation space. Comparison of the recently reported structures²⁰ of (1,3-*i*-Pr-indenyl)₂Ca·THF and (1,3-*i*-Pr-indenyl)₂Ba·THF with those of Me₂SiFl₂Ca·3THF and Me₂SiFl₂Ba·4THF, shows that the latter are more abundantly solvated by THF molecules. This is due partly to the Si bridge opening the gap available for solvation and partly to the tilting of the rings away from the metal cation.

Conclusions

The structures of Si-bridged fluorenyl metallocenes with Li, Ca, and Ba do not show the distortions that are typical for d- and f-block Si-bridged metallocenes. Rather, fluorenyl–metal coordination is observed to differ from η⁵-bonding. Instead of tilting the fluorenyl rings toward the metal in order to strengthen the metal coordination, the structures reported here generally show a tilting of the fluorenyl group away from the metal. This increases the electron density in the fluorenyl ring at the side of the metal cation and allows for a more extended solvation of the metal by external solvent molecules.

Experimental Section

General Methods. All experiments were carried out under argon using predried solvents and Schlenk techniques. ¹H and ¹³C NMR spectra were recorded on a Bruker AC250 (250 MHz) machine (reference TMS) and ⁷Li NMR spectra on a JEOL (400 MHz) machine (reference 1M LiBr in THF). All Me₂Si(fluorenyl)₂–metal compounds were prepared by reacting Me₂Si(fluorenyl-H)₂ with the corresponding metal–N(TMS)₂, since the only other byproduct, HN(TMS)₂, can be easily removed under high vacuum and/or washing with pentane. Me₂Si(fluorenyl-H)₂²¹ and Ca[N(TMS)₂]₂²² were prepared according to literature procedures. Ba[N(TMS)₂]₂ was prepared according to a modified literature procedure;²³ the crystalline Ba[N(TMS)₂]₂·2THF was freed from THF by heating the powdered crystals under vacuum (0.01 Torr, 90 °C, 5 h), rather than by sublimation. Crystal structure solution and refinement were performed with the programs SHELXS86²⁴ and SHELXL93.²⁵ Plots and geometry calculations were made with the EUCLID package.²⁶

Computational Methods. Geometries were fully optimized at the restricted Hartree–Fock level by using gradient optimization techniques and the standard basis set, 6-31+G*, incorporated in the GAUSSIAN 94 program system.²⁷ All stationary points were checked to be real minima by frequency analyses (no imaginary frequencies were found). Calculations on deformed structures have been performed by full optimization of the remaining variables within in the designated

symmetry restriction. Calculations on H₃Si(fluorenyl)[–] systems were carried out using the smaller 3-21G* basis set. Charges have been calculated by use of the natural population analysis.¹³

Synthesis of Me₂SiFl₂Li₂. Butyllithium (1.6 M in hexane, 2.0 mL) was added at once to a suspension of Me₂Si(fluorenyl-H)₂ (0.50 g, 1.29 mmol) in 10 mL of Et₂O. An orange solution resulted from which small yellow crystals precipitated. After 1 h, the solvent from the reaction mixture was removed under vacuum and the remaining solid was washed two times with 10 mL of pentane. The crude yellow-orange product was freed from Et₂O under vacuum (0.01 Torr, 60 °C, 30 min) and recrystallized from a hot mixture of hexane (10 mL) and THF (4 mL) yielding yellow crystals of [Me₂SiFl₂Li₂THF][–][Li·4THF]⁺ (0.55 g, 51%). ¹H-NMR (benzene-*d*₆, 20 °C): 1.15 (m, 12H, THF) 1.39 (s, 6H, Me₂Si) 2.71 (m, 12H, THF) 7.06 (t, ³J(H,H) = 7.1 Hz, 4H, Fl) 7.39 (t, ³J(H,H) = 6.9 Hz, 4H, Fl) 8.36 (d, ³J(H,H) = 7.7 Hz, 4H, Fl) 8.48 (d, ³J(H,H) = 8.1 Hz, 4H, Fl). ¹³C-NMR (benzene-*d*₆, 20 °C): 3.7 (Me₂Si) 25.7 and 67.7 (THF) 80.9, 112.1, 18.0, 19.6, 122.0, 127.7 and 143.3 (fluorenyl). ⁷Li-NMR (toluene-*d*₈, 20 °C): –3.54 (s). ⁷Li-NMR (toluene-*d*₈, –90 °C): –2.98 (s) –3.87 (s).

Synthesis of Me₂SiFl₂Ca. A solution of Ca[N(TMS)₂]₂ (0.39 g, 1.08 mmol) and Me₂Si(fluorenyl-H)₂ (0.39 g, 1.00 mmol) in 10 mL of toluene and 4 mL of THF was refluxed for 2 h. The solvent of the resulting orange solution was removed under vacuum, and the remaining solid was freed of HN(SiMe₃)₂ under vacuum (0.01 Torr, 60 °C, 1 h). The orange-red solid obtained was crystallized by dissolving it in a mixture of THF (7 mL) and hexane (7 mL) at +60 °C and cooling it slowly (within 24 h) to –20 °C. Yellow single-crystals of Me₂SiFl₂Ca·3THF were formed in an overall yield of 53% (0.34 g). The crystalline pure material is only very slightly soluble in THF. ¹H-NMR (THF-*d*₆, 20 °C): 0.89 (s, 6H, Me₂Si) 1.76 (m, 12H, THF) 3.63 (m, 12H, THF) 6.83 (t, ³J(H,H) = 7.2 Hz, 4H, Fl) 7.19 (t, ³J(H,H) = 7.3 Hz, 4H, Fl) 8.05 (d, ³J(H,H) = 8.0 Hz, 4H, Fl) 8.09 (d, ³J(H,H) = 8.0 Hz, 4H, Fl).

Synthesis of Me₂SiFl₂Ba. A solution of Ba[N(TMS)₂]₂ (0.50 g, 1.09 mmol) and Me₂Si(fluorenyl-H)₂ (0.42 g, 1.08 mmol) in 14 mL of THF was heated for 1 h at 60 °C. The solvent of the resulting orange solution was removed under vacuum, and the remaining foamy substance was freed of HN(SiMe₃)₂ under vacuum (0.01 Torr, 80 °C, 1 h). The orange-red solid obtained was recrystallized from hot THF (12 mL). Large orange blocks of Me₂SiFl₂Ba·4THF were formed in an overall yield of 58% (0.46 g). The crystalline pure material is only very slightly soluble in THF. ¹H-NMR (THF-*d*₆, 20 °C): 1.04 (s, 6H, Me₂Si) 1.77 (m, 12H, THF) 3.60 (m, 12H, THF) 6.73 (t, ³J(H,H) = 6.8 Hz, 4H, Fl) 7.12 (t, ³J(H,H) = 7.4 Hz, 4H, Fl) 7.98 (d, ³J(H,H) = 8.3 Hz, 4H, Fl) 8.03 (d, ³J(H,H) = 7.9 Hz, 4H, Fl).

Crystal Structure Data for 4. Monoclinic, *a* = 10.496(2) Å, *b* = 17.999(2) Å, *c* = 25.414(5) Å, β = 95.02(1)°, *V* = 4783-(1) Å³, space group *P*2₁/c, formula C₅₂H₇₀Li₂O₆Si, *M_w* = 833.1, *Z* = 4, ρ_{calcd} = 1.157 g cm^{–3}, μ(Mo Kα) = 0.096 mm^{–1}; 9170 reflections were measured (Mo Kα, graphite monochromator, *T* = –120 °C), 8392 unique reflections after merging (*R*_{int} = 0.050), 4567 observed reflections with *I* > 2.0σ(*I*). Solution by direct methods, full-matrix least-squares refinement on *F*² to *R*₁ = 0.067, *wR*₂ = 0.165 (629 parameters, 8328 data). Non-hydrogens were refined anisotropically. Part of the hydrogen atoms have been taken from the difference Fourier map, and the rest were calculated.

Crystal Structure Data for 5. Monoclinic, *a* = 9.916(2) Å, *b* = 20.727(2) Å, *c* = 16.891(4) Å, β = 95.54(1)°, *V* = 3455-

(20) Overby, J. S.; Hanusa, T. P. *Organometallics* **1996**, *15*, 2205.
(21) Chen, Y.-X.; Rausch, M. D.; Chien, J. C. W. *J. Organomet. Chem.* **1995**, *497*, 1.

(22) Westerhausen, M. *Inorg. Chem.* **1991**, *30*, 96.

(23) Vaartstra, B. A.; Huffman, J. C.; Streib, W. E.; Caulton, K. G. *Inorg. Chem.* **1991**, *30*, 121.

(24) Sheldrick, G. M. *SHELXS86, Crystallographic Computing 3*; Sheldrick, G. M., Krüger, C., Goddard, R., Eds.; Oxford, 1985.

(25) Sheldrick, G. M. *SHELXL93, Program for the refinement of Crystal Structures*; Universität Göttingen, Germany, 1993.

(26) Spek, A. L. *The EUCLID package, Computational Crystallography*; Sayre, D., Ed.; Clarendon Press: Oxford, England, 1982.

(27) Frisch, M. J.; Trucks, G. W.; Schlegel, H. B.; Gill, P. M. W.; Johnson, B. G.; Robb, M. A.; Cheeseman, J. R.; Keith, T. A.; Petersson, G. A.; Montgomery, J. A.; Raghavachari, K.; Al-Laham, M. A.; Zakrzewski, V. G.; Ortiz, J. V.; Foresman, J. B.; Cioslowski, J.; Stefanov, B. B.; Nanayakkara, A.; Challacombe, M.; Peng, C. Y.; Ayala, P. Y.; Chen, W.; Wong, M. W.; Andres, J. L.; Replogle, E. S.; Gomperts, R.; Martin, R. L.; Fox, D. J.; Binkley, J. S.; Defrees, D. J.; Baker, J.; Stewart, J. P.; Head-Gordon, M.; Gonzalez, C.; Pople, J. A. *GAUSSIAN 94*, Revision C.3; Gaussian Inc.: Pittsburgh, PA, 1995.

(1) Å³, space group $P2_1/n$, formula C₄₀H₄₆CaO₃Si, $M_w = 642.97$, $Z = 4$, $\rho_{\text{calcd}} = 1.236 \text{ g cm}^{-3}$, $\mu(\text{Mo K}\alpha) = 0.253 \text{ mm}^{-1}$; 8274 reflections were measured (Mo K α , graphite monochromator, $T = -120 \text{ }^\circ\text{C}$), 7811 unique reflections after merging ($R_{\text{int}} = 0.017$), 5521 observed reflections with $I > 2.0\sigma(I)$. Solution by direct methods, full-matrix least-squares refinement on F^2 to $R_1 = 0.042$, $wR_2 = 0.097$ (580 parameters, 7811 data). Non-hydrogens were refined anisotropically. Part of the hydrogen atoms have been taken from the difference Fourier map, and the rest were calculated.

Crystal Structure Data for 6. Triclinic, $a = 12.684(5) \text{ \AA}$, $b = 15.851(7) \text{ \AA}$, $c = 20.725(9) \text{ \AA}$, $\alpha = 102.82(2)^\circ$, $\beta = 106.43(2)^\circ$, $\gamma = 91.79(3)^\circ$, $V = 3877(3) \text{ \AA}^3$, space group $P\bar{1}$, formula C₄₄H₅₄BaO₄Si, $M_w = 812.31$, $Z = 4$, $\rho_{\text{calcd}} = 1.392 \text{ g cm}^{-3}$, $\mu(\text{Mo K}\alpha) = 1.097 \text{ mm}^{-1}$; 18 341 reflections were measured (Mo K α , graphite monochromator, $T = -120 \text{ }^\circ\text{C}$), 17 541 unique reflections after merging ($R_{\text{int}} = 0.025$), 13 493 observed reflections with $I > 2.0\sigma(I)$. Solution by direct methods, full-matrix least-squares refinement on F^2 to $R_1 = 0.037$, $wR_2 = 0.106$ (1333 parameters, 17 522 data). Non-hydrogens were refined aniso-

tropically. Part of the hydrogen atoms have been taken from the difference Fourier map, and the rest were calculated.

Acknowledgment. S.H. thanks the European Community for a Human Capital and Mobility fellowship. Prof. Dr. H.-H. Brintzinger and Prof. Dr. G. Müller are kindly acknowledged for helpful discussions and for providing laboratory facilities.

Supporting Information Available: Tables of crystal data and structure refinement, atomic coordinates and isotropic displacement parameters, bond lengths and angles, anisotropic displacement parameters, and hydrogen coordinates and isotropic displacement parameters for Me₂Si(fluorenyl)₂Ba·4THF, Me₂Si(fluorenyl)₂Ca·3THF, and Me₂Si(fluorenyl)₂Li₂·6THF (30 pages). Ordering information is given on any current masthead page.

OM960587J